Appl. Phys. A 72 [Suppl.], S253–S256 (2001) / Digital Object Identifier (DOI) 10.1007/s003390100661

Applied Physics A
Materials
Science & Processing

An ultralow-temperature scanning tunnelling microscope

M.D. Upward[1], **J.W. Janssen**[1,*], **L. Gurevich**[1,2,**], **A.F. Morpurgo**[1,2,**], **L.P. Kouwenhoven**[1,2,**]

[1] Department of Applied Physics, Delft University of Technology, Lorentzweg 1, 2628 JD Delft, The Netherlands
[2] ERATO Mesoscopic Correlation Project

Received: 19 July 2000/Accepted: 14 December 2000/Published online: 11 April 2001 –

Abstract. We have developed a home-built ultralow-temperature scanning tunnelling microscope (STM) capable of continuous operation down to 70 mK, and in a magnetic field of up to 12 T. Extensive testing has shown that the STM is capable of very stable operation, including atomic resolution and spectroscopy with a high energy resolution. To test the microscope we have investigated the structural and electronic properties of the type-II superconductor $NbSe_2$.

PACS: 61.16.Ch; 75.25.Jb; 74.60.-w

The STM, since its development in 1982 [1, 2], has been adapted for operation in a wide variety of conditions, for instance ultrahigh vacuum, high temperatures and very low temperatures. Microscopes that operate at very low temperatures, particularly in the milliKelvin regime, have been the subject of a great deal of recent interest. Such instruments enable phenomena that have critical temperatures below 1 K to be investigated with the inherently high spatial resolution of STM. Operation at these temperatures can also provide high energy resolution, which ideally is just limited by thermal broadening. STM is also unique in its ability to measure the spatial variation of the local density of states (LDOS) with atomic resolution. To date there have been relatively few reports of STMs capable of operating at temperatures below 1 K [3–5] and even fewer capable of less than 100 mK [6, 7]. This is primarily due to the technical difficulties associated with combining the two techniques.

In this paper we present the design and testing of a STM attached to a dilution refrigerator that is capable of operating at 70 mK. The system is also equipped with a 12 T superconducting magnet. This combination of low temperatures and magnetic field is useful for the study of low-T_C superconductors and any material where spin plays an important role.

*Corresponding author.
(Fax: +31-15-2617868, E-mail: jorg@qt.tn.tudelft.nl)
**Also at ERATO Mesoscopic Correlation Project.

SPS 2000 – Second International Conference on Scanning Probe Spectroscopy, July 19–22, 2000 in Hamburg, Germany

1 Design

Our design is based upon a modified Oxford Instruments Kelvinox 100 dilution refrigerator. The STM head is home-built and its design has been reported previously [8]. Figure 1 is a schematic diagram of the head illustrating the principal features. Briefly, the scanning piezo-tube[1] (Fig. 1A) is mounted inside a polished cylinder (Fig. 1B), referred to from now on as the plunger, which is coated with a hard ceramic layer. This can slide vertically inside a second cylinder (Fig. 1C) which has been cut to produce two leaf springs,

[1] PZT5H piezoelectric tubes supplied by Morgan Matroc Inc.; scan tube: 12.6 mm long, 6.35 mm diameter, 0.7 mm wall thickness; coarse-approach tube: 12.7 mm long, 15.6 mm diameter, 0.8 mm wall thickness.

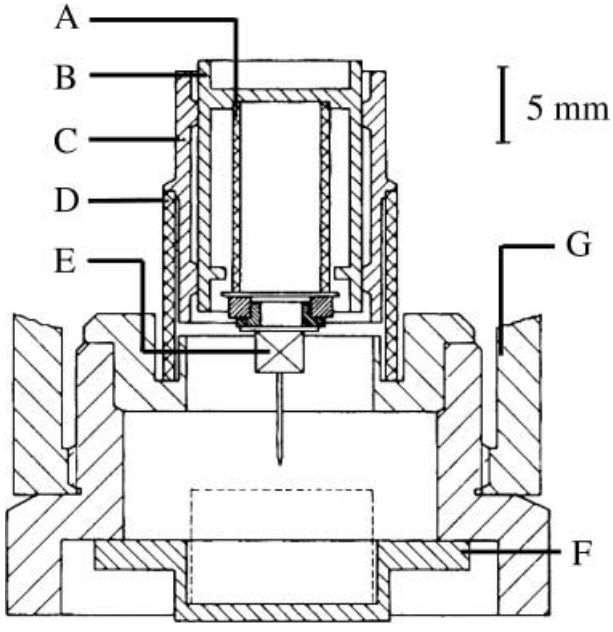

Fig. 1. Design of the STM head: (A) scan piezo-tube, (B) plunger, (C) leaf spring, (D) outer coarse-approach piezo, (E) tip holder, (F) sample holder, (G) STM body

which grip the plunger. This whole assembly is glued to a large piezo-tube (Fig. 1D) using epoxy[2]. When high-voltage pulses of a carefully chosen shape are applied to this piezo the plunger moves up or down with a slip-stick motion. This scan tube gives a maximum scan area of $1 \times 1\ \mu m^2$ at low temperatures. We are able to remove this plunger and replace it with a different one incorporating a longer tube if larger scan areas are required. We do not have the capability of controlled x or y coarse motion. However, we have found that we can move to a random new area by retracting a large number of steps and then reapproaching. We believe that this is due to a small rotation of the plunger while moving.

The design of the STM head is very compact, a cylinder 30 mm in diameter and 58 mm high. This small size is required so that the STM can fit inside the bore of our superconducting magnet. The STM screws onto the bottom of the cold finger attached to the mixing chamber of the dilution refrigerator. The body of the STM is made of copper to provide efficient cooling, and has a large contact area with the cold finger. A calibrated ruthenium oxide resistor attached to the bottom of the mixing chamber is used to measure the temperature. The entire STM is unscrewed and removed to aid sample and tip changing. We operate the STM using control electronics and software supplied by RHK Technology Inc. (SPM 100), a home-built I–V converter and an EG&G preamplifier. All of the wires entering the cryostat are RF filtered at room temperature.

The sensitivity of a STM to vibrations requires that the head and insert are made as mechanically stiff as possible. Vibration isolation is provided by suspension of the dewar and insert from elastic ropes that are attached to the ceiling. All the pumps for the system are located in the basement below and are electrically isolated and vibrationally decoupled by using flexible pipes. In addition, the circulation pumping lines are also fed through a heavy sand-filled box for further isolation. When a magnetic field is used the magnet is always operated in persistent-current mode so that the heavy-current leads can be disconnected, as they are a possible source of vibrations. The stability of our measurements, including atomic resolution (see Fig. 2), shows that these vibration-isolation measures are very successful.

To remove the need to disconnect all the wiring and pipes each time the insert needs to be removed from the dewar, we have a system whereby the insert is attached to a frame and the dewar is lowered through the floor. This also speeds up the time that it takes to cool down the insert, as the circulation pipes remain pumped at all times. After raising the dewar and filling with liquid helium it takes approximately 1 h for the insert to cool down to 4.2 K. The inner vacuum can is then pumped to remove the exchange gas before the circulation is started. The whole procedure to go from base temperature to room temperature, changing the tip and sample and returning to base temperature can be done in less than 24 h.

[2] Stycast is a product of Emerson and Cuming Inc. We have used Stycast 2850FT.

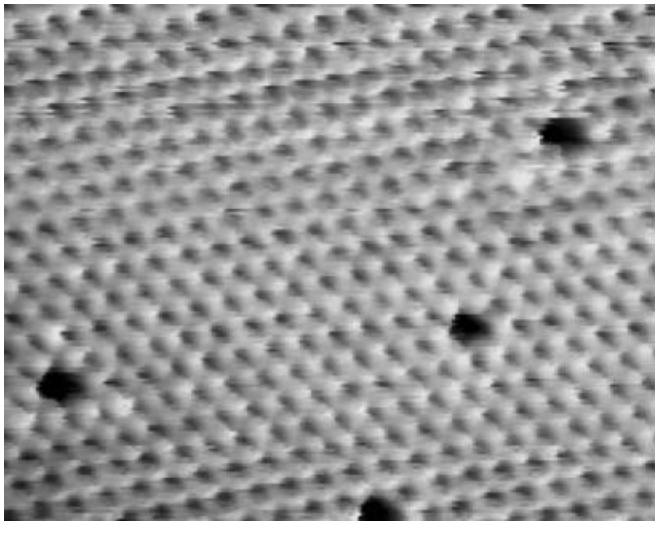

Fig. 2. Unfiltered 7×5.6 nm atomically resolved constant-current image of $NbSe_2$ acquired at 190 mK

2 Experimental results

The initial experiments to obtain atomic resolution were performed at room temperature using highly oriented pyrolytic graphite. After their successful conclusion we moved on to testing at low temperature. We chose 2H–$NbSe_2$ to provide a means of testing the imaging and spectroscopic capabilities of the STM. This material has been extensively studied in the past [9]. It has a charge density wave and is a superconductor with a T_C of 7.2 K. $NbSe_2$ is a type-II superconductor, so upon application of a sufficiently large magnetic field an Abrikosov vortex lattice is produced. This allows us to test the magnet in the system. In addition, $NbSe_2$ is inert and is easy to cleave to produce large flat areas. For these experiments the samples were cleaved at room temperature and in air just prior to mounting in the STM.

Figure 2 is an atomically resolved image of $NbSe_2$ at 190 mK. This image was acquired in constant-current mode and is shown here with no filtering. The four black circles are missing single surface atoms. This image demonstrates the low level of vibrational noise in the system. One of the main reasons for operating at low temperatures is the possibility for a high energy resolution. To test these spectroscopic capabilities we measured the differential conductance spectra of $NbSe_2$ using a standard lock-in technique. The ac signal applied during these measurements was typically $14\ \mu V_{rms}$. We have also been able to measure spectra using a $7\ \mu V_{rms}$ modulation. Figure 3a shows the differential conductance spectrum measured on $NbSe_2$ with a sample temperature of 210 mK. Ideally we would like to use this spectrum, which has clear peaks and an energy gap characteristic of BCS superconductors, to calculate the effective electron temperature, T_{eff}, of the microscope. However, $NbSe_2$ has an anisotropic superconducting energy gap, Δ, varying between 0.7 and 1.4 mV [9] depending on the crystal direction (or $\underline{\boldsymbol{k}}$-vector). The curves cannot therefore be fitted to provide a precise value of the effective temperature. This is illustrated by the gradient of the edge of the gap (Fig. 3a), which in a BCS superconductor would be a vertical line broadened by the effective temperature only. Nevertheless, from these measurements we estimate our effective temperature to be close to that measured by Moussy et al. [7], who found $T_{eff} = 210$ mK with a sample temperature of 60 mK. We are currently repro-

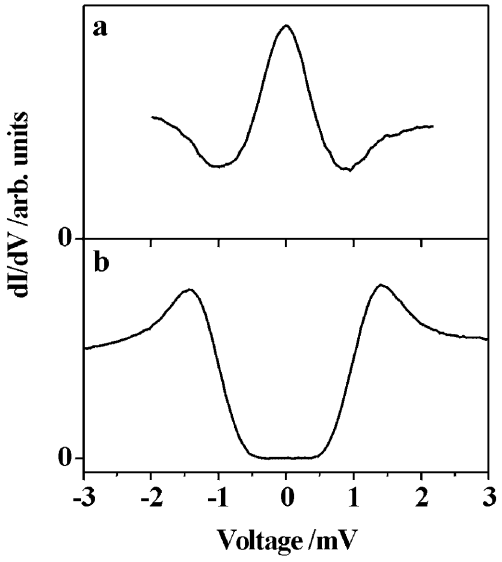

Fig. 3. a Differential conductance spectrum of superconducting $NbSe_2$ acquired after stabilising the feedback at 40 pA and +4 mV at a temperature of 210 mK. (This curve is an average of 128 individual curves.) **b** Differential conductance spectrum acquired in the centre of a vortex at 0.2 T and 110 mK after stabilising the feedback at 50 pA and +3.5 mV

ducing their experiment to determine a more precise value of T_{eff}.

To test our superconducting magnet we applied a magnetic field perpendicular to the sample. Since $NbSe_2$ is a type-II superconductor, the field penetrates the sample and an Abrikosov flux lattice is formed. An image of this flux lattice is shown in Fig. 4. Figure 3b is a differential conductance spectrum measured in the centre of a flux vortex, which exhibits a zero bias peak in the density of states. This feature was first observed by Hess et al. [9] and has been attributed to quasiparticle bound states within the "potential well" formed by the vortex [10]. The image in Fig. 4 was acquired by recording the signal from the lock-in amplifier while scanning with a sample bias of 1.3 mV. At a bias of ~ 1.3 mV the $\mathrm{d}I/\mathrm{d}V$ signal in the centre of the vortex is smaller than the $\mathrm{d}I/\mathrm{d}V$ signal in the superconducting region and the vortices appear as dark depressions in the image. For a thorough discussion of the relationship between the measured $\mathrm{d}I/\mathrm{d}V$ and the LDOS in a vortex core we refer the reader to the work of Hess et al. [9].

In many cases it is interesting to measure and map the variation of the LDOS across the sample at a particular bias rather than measure the LDOS versus energy at an individual point. To test this type of measurement we measured the spatial distribution of the quasiparticle density of states around 0 V. This can not be done with a straightforward scanning technique, so a different method is used where at each spatial point the tip is stabilised at a voltage above the gap energy and the feedback loop disengaged. The differential conductance is then measured over a small bias range around 0 V. Finally, the data point for each different bias setting is extracted from each curve and converted to a colour scale to produce an image. One such image using this technique is shown in Fig. 5. White represents a high and black a low conductance. To enhance the appearance of the shape of various critical features black lines have been added at periodic intervals to this grey scale, resulting in contour-like shapes. The whitest areas, one of which has been highlighted with a white circle, are the peaks in the LDOS at the vortex cores. The darkest areas, highlighted with white ovals, are superconducting regions. It is immediately noticeable that the vortex core is not completely surrounded by a superconducting region; there is a 6-fold star pattern (that has been highlighted by white lines). Our observations reproduce those of Hess et al. [9] and have been explained by includ-

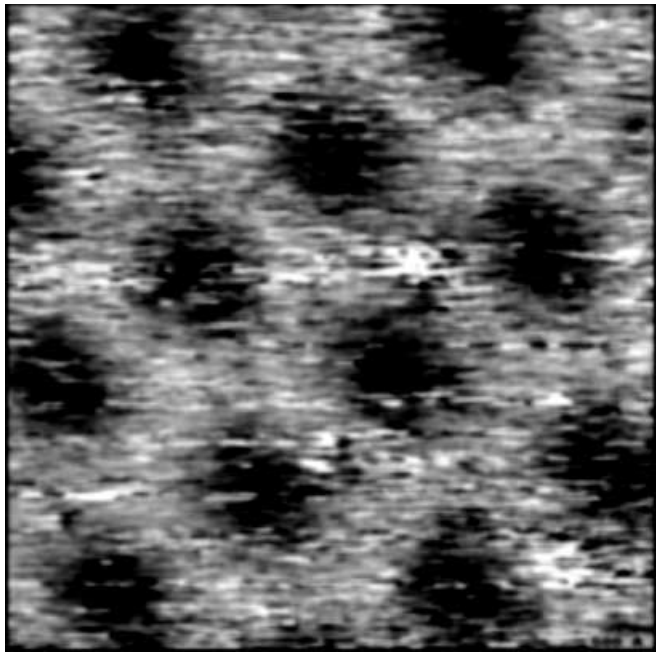

Fig. 4. 500×500 nm image of the Abrikosov flux lattice formed with a 0.5 T field applied perpendicular to the sample

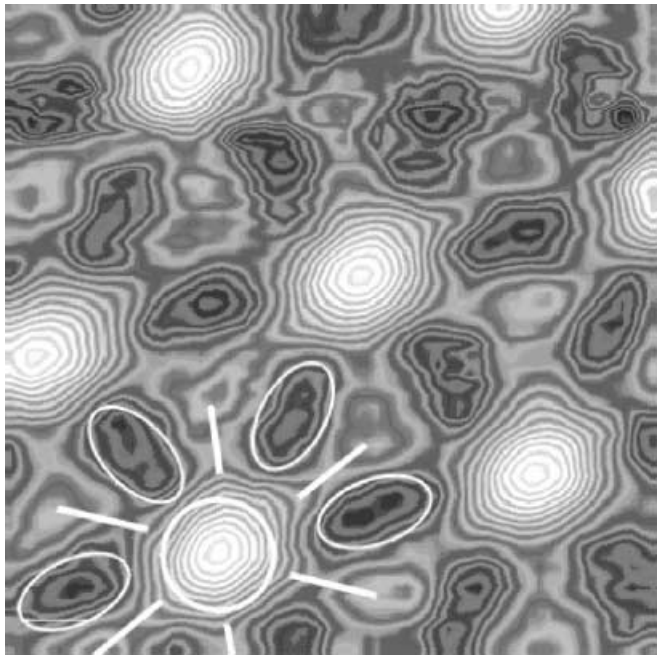

Fig. 5. Real-space image of the local density of states at 0 V of a 400×400 nm area containing seven vortices, measured at 0.4 T and 125 mK

ing effects from an anisotropic LDOS and an anisotropic pairing [11].

3 Conclusions

We have developed a STM attached to a dilution refrigerator operating at 70 mK. We have demonstrated the high-quality imaging and spectroscopic capabilities of this instrument. Magnetic fields of up to 12 T can be applied perpendicular to the sample. The combination of low temperatures and a high magnetic field allows investigations of a variety of phenomena including the regime where the Zeeman spin splitting exceeds the thermal broadening ($g\mu_{\mathrm{B}}B > kT$). We are currently pursuing experiments on the properties of unconventional superconductors such as the borocarbides and strontium ruthenates.

Acknowledgements. The authors would like to thank J.W.G. Wildöer, R. Schouten, L. Canali, M. Janus, C.J.P.M. Harmans, C. van der Wal, T.H. Oosterkamp and B. van der Enden, for their help. We acknowledge financial support from the Dutch Organisation for Fundamental Research on Matter (FOM) and from the NEDO joint research programme NTDP-98.

References

1. G. Binning, H. Rohrer, C. Gerber, E. Weibel: Phys. Rev. Lett. **40**, 178 (1982)
2. G. Binning, H. Rohrer, C. Gerber, E. Weibel: Appl. Phys. Lett. **49**, 57(1982)
3. H. Fukuyama, H. Tan, T. Handa, T. Kumakura, M. Morishita: Czech. J. Phys. **46**, Suppl. S5 2847 (1996)
4. S.H. Pan, E.W. Hudson, J.C. Davis: Rev. Sci. Instrum. **70**, 1459 (1999)
5. M. Kugler, C. Renner, Ø. Fisher, V. Mikheev, G. Batey: Rev. Sci. Instrum. **71**, 1475 (2000)
6. H.F. Hess, R.B. Robinson, J.V. Waszczak: Phys. Rev. Lett. **64**, 2711 (1990)
7. N. Moussy, H. Courtois, B. Pannetier: Submitted to Rev. Sci. Instrum.
8. J.W.G. Wildoer, A.J.A. van Roy, H. van Kempen, C.J.P.M. Harmans: Rev. Sci. Instrum. **65**, 2849 (1994)
9. H.F. Hess, R.B. Robinson, R.C. Dynes, J.M. Valles, Jr., J.V. Waszczak: Phys. Rev. Lett. **62**, 214 (1989); H.F. Hess, R.B. Robinson, J.V. Waszczak: Physica B: **169**, 422 (1991) and references therein
10. A.W. Overhauser, L.L. Daemen: Phys. Rev. Lett. **62**, 1691 (1989); L.L. Daemen, A.W. Overhauser: Phys. Rev. B **40**, 10778 (1989); J.D. Shore, M. Huang, A.T. Doresy, J.P. Sethna: Phys. Rev. Lett. **62**, 3089 (1989); F. Gygi, M. Schlüter: Phys. Rev. B **41**, 822 (1990)
11. F. Gygi, M. Schlüter: Phys. Rev. Lett. **65**, 1820 (1990); N. Hayashi, M. Ichioka, K. Machida: Phys. Rev. Lett. **77**, 4074 (1996)